

Non-diffusion theory of weak localization in graphene

M.O. Nestoklon, N.S. Averkiev

Ioffe Physical-Technical Institute, Russian Academy of Sciences, St. Petersburg 194021, Russia

We put forward a theory of the weak localization in two dimensional graphene layers which explains experimentally observable transition between positive and negative magnetoresistance. Calculations are performed for the whole range of classically weak magnetic field with account on intervalley transitions. Contribution to the quantum correction which stems from closed trajectories with few scatterers is carefully taken into account. We show that intervalley transitions lead not only to the transition from weak antilocalization to the weak localization, but also to the non-monotonous dependence of the conductivity on the magnetic field.

PACS numbers: 72.15.Rn, 72.80.Vp, 81.05.ue

I. INTRODUCTION

Recent studies of perfect graphene layers gave a new impulse^{1,2} for experimental and theoretical investigation of two- and three-dimensional structures with linear energy spectrum of the carriers. Despite the differences in chemical bonding, electrical properties of graphene layers, surface states in Bi₂Se₃, Bi₂Te₃, Bi₂Te₂Se and quantum wells based on HgTe are defined mostly by the linear energy dependence on lateral wave vector. This dependence leads to weak antilocalization (WAL) and positive magnetoresistance in classically weak magnetic fields if all relaxation processes take place inside one dispersion cone.³⁻⁵ As long as zero energy in graphene is located at the Brillouin zone boundary in K point in contrast to topological insulators, significant role in transport phenomena is also played by intervalley transitions between equivalent points K and K' . When considering the intervalley transitions, it is important to take into consideration that valleys in graphene are connected by time inversion. It leads⁶⁻⁸ to weak localization (WL) when the phase relaxation time τ_ϕ in each valley is larger than intervalley transition time τ_v . The ratio τ_ϕ/τ_v in graphene may be controlled by changing the gate bias. Previous theoretical investigations considered either non-diffusion theory with account on intervalley transitions in zero magnetic field⁸ or magnetoresistance in diffusion regime.^{7,9} Experimentally, magnetoresistance has been extensively studied¹⁰⁻¹² and it has been shown that both (WAL and WL) regimes are possible depending on technology of sample and applied bias.

Weak localization phenomenon is based on the change of carrier return probability due to interference of the waves travelling the same path in the opposite directions. Magnetic field applied to the structure or other processes of the phase decoherence change the interference conditions which results in changing the contribution to the conductivity from the closed trajectories. As long as the magnetic field which changes the phase is classically weak and the change of wavefunction phase is quantum phenomenon, such corrections are normally called quantum corrections.

Intervalley transitions were considered in the frame-

work of diffusion approximation for graphene⁷ and for tellurium which has similar bandstructure.¹³ These results show that transition from antilocalization to localization regime in graphene is possible when $3 \ln(\tau_v/\tau_\phi) > 2 \ln(\tau_\phi/\tau_{tr})$ (here τ_{tr} is momentum relaxation time). Both terms should be significantly large than unity. The diffusion theory describes the quantum correction to the conductivity in the limit $\ln(\tau_\phi/\tau_{tr}) \gg 1$ assuming that this it is relatively easy to go beyond this regime in highly conducting samples. To overcome this limitation in theory it is necessary to include into consideration closed paths with small number of scatterers. Movement along such trajectories is non-diffusion. As long as in reality both $\ln(\tau_v/\tau_\phi)$ and $\ln(\tau_\phi/\tau_{tr})$ are less than 10, diffusion theory may give only qualitative estimation of the quantum correction and one may not use its results to analyze the magnetoresistance caused by the weak localization.

The weak localization regime is known to be protected by the time inversion.⁹ In the system where carriers are located near Γ point of Brillouin Zone the time inversion guarantees the diffusion pole for the Cooperons because the correlator in self-energy part coincides with the correlator in Cooperon equation. In multivaley systems where the valleys are connected by time inversion (see e.g. Ref. 14) time inversion guarantees diffusion pole for intervalley Cooperons only. For diffusion pole for intravalley Cooperons additional symmetries (in graphene space inversion inside one valley^{7,9}) are needed.

Generalization of the theory of magnetic field quantum corrections to the non-diffusion case appears to be the last conceptual theoretical problem of the weak localization theory in graphene. This theory may also be considered as a limit case of strong spin-orbit interaction (of Rashba or Dresselhaus type) in two-dimensional electron systems,¹⁵ when linear in \mathbf{k} terms in Hamiltonian dominate. The goal of this work is the theoretical study of the weak localization in graphene in the full range of classically weak magnetic fields.

The manuscript is organized as follows: Section II gives an extended introduction in the weak localization in graphene. In section III we give some details of the non-diffusion calculations of the weak localization: we start from the main starting points of the theory, choice

of basis functions, Hamiltonian, scattering matrix elements, etc. In subsection III A we derive the Green function in two valleys in real space, in subsection III B we write and solve Cooperon equation, subsection III C gives the derivation of equations for weak localization corrections. Subsection III D gives low magnetic field limit of the results obtained before. Finally, in section IV we present the results of the weak localization correction computations. In addition, in appendix A we give important details of numerical calculation of integrals which arise in computation of weak localizations correction, appendix B gives a recipe to simplify calculation of infinite sums for the weak localization correction and finally appendix C gives some mathematical relations used in the manuscript.

II. QUALITATIVE ANALYSIS OF THE WEAK (ANTI)LOCALIZATION

The intra-valley electron scattering from a symmetric short-range (as compared to de Broglie wavelength) impurity in graphene is described by the matrix element of scattering

$$V(\mathbf{k}', \mathbf{k}) \propto e^{i(\varphi - \varphi')/2} \cos[(\varphi - \varphi')/2], \quad (1)$$

where $\mathbf{k} = (k \cos \varphi, k \sin \varphi)$ and $\mathbf{k}' = (k \cos \varphi', k \sin \varphi')$ are wave vectors of respectively incident and scattered electrons.

One can see that the direct back scattering from an impurity is suppressed and, what is more important for quantum effects, the scattering introduces the phase $(\varphi - \varphi')/2$ to the electron wave function. Therefore, an electron traveling clockwise along a closed path and finally scattered back gains the additional phase $\pi/2$ while the electron traveling in the opposite direction gains the phase $-\pi/2$. The phase shift of π between these two waves results in a destructive interference and, hence, in the antilocalization of carriers.

Other forms of scattering amplitude lead to the phase gain which depends on the particular trajectory even for closed paths. Averaging over the trajectories destroys the wave interference and results in no quantum corrections to conductivity (see Refs. 7, 16, and 17). It is a general rule which manifests itself in a fact that corrections to electron Hamiltonian due to e.g. trigonal warping, non-symmetric scattering, etc. in graphene suppress the weak antilocalization.⁷

In the system where carriers are located near Γ point of Brillouin Zone the time inversion guarantees the diffusion pole for the intravalley Cooperons as long as correlator in self-energy part coincides with the correlator in Cooperon equation. In multivalley systems where the valleys are connected by time inversion (see e.g. Ref. 14) time inversion guarantees diffusion pole only for intervalley Cooperons which do not contribute to conductivity in the absence of intervalley transitions. For diffusion pole for intravalley Cooperons other symmetries (in

graphene space inversion inside one valley^{7,9}) are needed. In the presence of intervalley scattering, Cooperons associated with such scattering contribute to conductivity giving rise to weak localization.^{7,8}

Intervalley contribution to the conductivity due to its time-invariant nature results in a conventional WL, as in spinless single valley case. However, it is proportional to the intervalley scattering rate. Changing intervalley scattering rate one may continuously switch between two cases.⁶⁻⁸

III. THEORY

In the following we work in the basis $\{KA, KB, K'B, K'A\}$ with basis functions KA, KB in one valley transform as $x \pm iy$ and the basis functions in the second valley are obtained by C_2 rotation perpendicular to graphene sheet.¹⁸ In this basis Hamiltonian is

$$\mathcal{H} = \hbar v \begin{pmatrix} \boldsymbol{\sigma} \cdot \mathbf{k} & 0 \\ 0 & -\boldsymbol{\sigma} \cdot \mathbf{k} \end{pmatrix}. \quad (2)$$

In the magnetic field, we neglect zeeman-like terms which do not contribute to the weak localization and the Hamiltonian reads

$$\mathcal{H} = \hbar v \frac{\sqrt{2}}{\ell_B} \begin{pmatrix} 0 & a_- & 0 & 0 \\ a_+ & 0 & 0 & 0 \\ 0 & 0 & 0 & -a_- \\ 0 & 0 & -a_+ & 0 \end{pmatrix}, \quad (3)$$

where we defined standard ladder operators $a_{\pm} = \ell_B(k_x \pm ik_y)/\sqrt{2}$, and ℓ_B is magnetic length. This Hamiltonian gives us the positive energy solutions in two valleys:

$$\begin{aligned} \Psi_{N,k,1}(\mathbf{r}) &= \frac{1}{\sqrt{2}} \begin{pmatrix} \psi_{N-1,k}(\mathbf{r}) \\ \psi_{N,k}(\mathbf{r}) \\ 0 \\ 0 \end{pmatrix}, \\ \Psi_{N,k,2}(\mathbf{r}) &= \frac{1}{\sqrt{2}} \begin{pmatrix} 0 \\ 0 \\ \psi_{N-1,k}(\mathbf{r}) \\ -\psi_{N,k}(\mathbf{r}) \end{pmatrix}. \end{aligned} \quad (4)$$

where $\psi_{N,k}$ are functions of electron in magnetic field in Landau gauge

$$\begin{aligned} \psi_{N,k}(\mathbf{r}) &= \frac{e^{iky - \frac{(x + \ell_B^2 k)^2}{2\ell_B^2}}}{\sqrt{\ell_B} \sqrt{2^N N!} \sqrt{\pi}} H_N \left(\frac{x + \ell_B^2 k}{\ell_B} \right), \\ H_N(\xi) &= (-1)^N e^{\xi^2} \frac{d^N}{d\xi^N} e^{-\xi^2} \end{aligned} \quad (5)$$

$$\begin{aligned} a_+ \psi_{N-1,k}(\mathbf{r}) &= \sqrt{N} \psi_{N,k}(\mathbf{r}), \\ a_- \psi_{N,k}(\mathbf{r}) &= \sqrt{N} \psi_{N-1,k}(\mathbf{r}) \end{aligned} \quad (6)$$

Scattering may be obtained from symmetry considerations. Assuming the non-magnetic potential with symmetry Γ_1^+ in Koster notation¹⁹ with the center at \mathbf{r}_0 it reads as

$$\delta\mathcal{H}_{intra}(\mathbf{r}; \mathbf{r}_0) = \sqrt{\frac{2v}{nk_F\tau}} \begin{pmatrix} 1 & 0 & 0 & 0 \\ 0 & 1 & 0 & 0 \\ 0 & 0 & 1 & 0 \\ 0 & 0 & 0 & 1 \end{pmatrix} \delta(\mathbf{r} - \mathbf{r}_0), \quad (7a)$$

$$\delta\mathcal{H}_{inter}(\mathbf{r}; \mathbf{r}_0) = \sqrt{\frac{2v}{nk_F\tau_v}} \begin{pmatrix} 0 & 0 & \varepsilon & 0 \\ 0 & 0 & 0 & \varepsilon \\ \varepsilon^* & 0 & 0 & 0 \\ 0 & \varepsilon^* & 0 & 0 \end{pmatrix} \delta(\mathbf{r} - \mathbf{r}_0), \quad (7b)$$

where τ is quantum relaxation time and $\varepsilon = e^{i(\mathbf{K}-\mathbf{K}')\cdot\mathbf{r}_0}$ is a phase which stems from difference of valley positions in k -space.

Note that in Ref. 8 authors omitted phase factor which takes into account position of impurity.

A. Green function

Without account on scattering, the Green function reads

$$G_0^{R,A}(\mathbf{r}, \mathbf{r}') = \sum_{N,k,t} \frac{\Psi_{N,k,t}(\mathbf{r})\Psi_{N,k,t}^+(\mathbf{r}')}{E_F - \varepsilon_N \pm i\frac{\hbar}{2\tau_\phi}} \quad (8)$$

Here t is valley index.

Solution of the Dyson equation for the renormalized Green function for the given short range scatterers (7) in the first order of scatterers density reads as

$$G^{R,A}(\mathbf{r}, \mathbf{r}') = \sum_{N,k,t} \frac{\Psi_{N,k,t}(\mathbf{r})\Psi_{N,k,t}^+(\mathbf{r}')}{E_F - \varepsilon_N \pm i\frac{\hbar}{2\tau'}} \quad (9)$$

where effective relaxation time $1/\tau' = 1/\tau_\phi + 1/\tau + 1/\tau_v$ is defined by harmonic sum of phase relaxation time τ_ϕ , quantum relaxation time τ and intervalley transition time τ_v .

With the help of results presented in Appendix C assuming $k_F\ell \gg 1$ (where $k_F = E_F/\hbar v$ is wave vector at Fermi level) in classically weak magnetic fields $k_F\ell_B \gg 1$ at sufficiently small distances the effect of the magnetic field on a Green function may be written as a phase factor:

$$G^{R,A}(\mathbf{r}, \mathbf{r}') = \exp\left[-i\frac{(x+x')(y-y')}{2\ell_B^2}\right] G_{B0}^{R,A}(\mathbf{r} - \mathbf{r}'), \quad (10)$$

where $G_{B0}^{R,A}(\mathbf{r} - \mathbf{r}')$ are the Green functions of an electron in graphene at zero field,

$$G_{B0}^{R,A}(\boldsymbol{\rho}) = -\frac{\exp[-\rho/(2\ell') \pm i(k_F\rho + \pi/4)]}{\sqrt{2\pi\rho/k_F\hbar v}} g^{R,A}(\boldsymbol{\rho}), \quad (11)$$

$$C^{(2)} = SPS + SPSPS + \dots = SP \cdot \left(\sum_{n=0}^{\infty} S(PS)^n \right) = SP \cdot C$$

FIG. 1. Illustration of the Cooperon equation

$$g^{R,A}(\boldsymbol{\rho}) = \frac{1}{2} \begin{pmatrix} 1 & \pm in_- & 0 & 0 \\ \mp in_+ & 1 & 0 & 0 \\ 0 & 0 & 1 & \mp in_- \\ 0 & 0 & \pm in_+ & 1 \end{pmatrix},$$

$\ell' = \ell / (1 + \tau/\tau_\phi + \tau/\tau_v)$, $\ell = v\tau$ is the mean free path.

B. Cooperon equation

The key point in calculation of the weak localization correction is the solution of Cooperon equation which describes the sum of the fan diagrams (see Fig. 1). As we have a complicated structure of the Green function, to simplify the solution we rewrite Cooperon equation in the matrix form.

We start from writing Cooperon equation in real space:

$$C_{\gamma\delta}^{\alpha\beta}(\mathbf{r}, \mathbf{r}') = S_{\gamma\delta}^{\alpha\beta}(\mathbf{r})\delta(\mathbf{r}-\mathbf{r}') + \int [SP]_{\gamma\xi}^{\alpha\zeta}(\mathbf{r}, \mathbf{r}'') C_{\xi\delta}^{\zeta\beta}(\mathbf{r}'', \mathbf{r}') d\mathbf{r}'', \quad (12)$$

where

$$P_{\gamma\delta}^{\alpha\beta}(\mathbf{r}, \mathbf{r}') = G_{\alpha\beta}^A(\mathbf{r}, \mathbf{r}') G_{\gamma\delta}^R(\mathbf{r}, \mathbf{r}') \quad (13)$$

and scattering correlator

$$\langle \delta\mathcal{H}_{\alpha\zeta}(\mathbf{r} - \mathbf{r}_1) \delta\mathcal{H}_{\gamma\xi}(\mathbf{r}' - \mathbf{r}_2) \rangle_{\mathbf{r}_1, \mathbf{r}_2} = S_{\gamma\xi}^{\alpha\zeta} \delta(\mathbf{r} - \mathbf{r}'). \quad (14)$$

It is not convenient to solve Cooperon equation in this form. To solve it efficiently we have to transform it into matrix equation.

To transform summation over two indices into standard matrix multiplication one needs to assume definite basis in direct product space. Below we use convention given in Table I. To distinguish between equations written in original and direct product spaces, later we use Greek letter indices for original space of graphene Hamiltonian and Latin letter indices for direct product space. For the Cooperon equation (see later) it is more convenient to rewrite scattering in product space. As a general rule, we rewrite each four-tail diagram with four indexes associated with four tails with a block having two indices each associated with a pair of tails: one to the left and one to the right, see Fig. 2.

Following this rule, we associate a correlator for the

TABLE I. Basis of direct product used in paper. Minus in the table is a shorthand for $|i\rangle = -|\alpha\rangle|\beta\rangle$.

α	1	1	2	2	1	1	2	2	3	3	4	4	3	3	4	4
γ	1	2	1	2	3	4	3	4	1	2	1	2	3	4	3	4
i	1	2	3	4	5	-6	7	-8	9	10	-11	-12	13	-14	-15	16

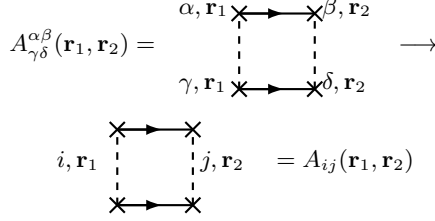


FIG. 2. Illustration of replacement of four-tail diagram with a block with two indexes in product space. Here $\alpha_\gamma \rightarrow i$, $\beta_\delta \rightarrow j$

pair of scatterings with the matrix

$$S_{ij} = W \cdot \begin{pmatrix} 1 & 0 & 0 & 0 \\ 0 & 1 & -\Pi_v \frac{\tau}{\tau_v} & 0 \\ 0 & -\Pi_v \frac{\tau}{\tau_v} & 1 & 0 \\ 0 & 0 & 0 & 1 \end{pmatrix}, \quad (15)$$

$$W = \frac{\hbar^2 v}{k_F \tau}, \quad (16)$$

The Cooperon equation separates into equations for intravalley contribution

$$C_0(\mathbf{r}, \mathbf{r}') = W\delta(\mathbf{r} - \mathbf{r}') + \int P_{sv}(\mathbf{r}, \mathbf{r}') C_0(\mathbf{r}'', \mathbf{r}') d\mathbf{r}'', \quad (20a)$$

and two intervalley equations

$$C_1(\mathbf{r}, \mathbf{r}') = W\delta(\mathbf{r} - \mathbf{r}') + \int P_{sv}(\mathbf{r}, \mathbf{r}') C_1(\mathbf{r}'', \mathbf{r}') d\mathbf{r}'' + \frac{\tau}{\tau_v} \Pi_v \int P_{sv}(\mathbf{r}, \mathbf{r}') C_2(\mathbf{r}'', \mathbf{r}') d\mathbf{r}'' \quad (20b)$$

$$C_2(\mathbf{r}, \mathbf{r}') = \frac{\tau}{\tau_v} \Pi_v W\delta(\mathbf{r} - \mathbf{r}') + \int P_{sv}(\mathbf{r}, \mathbf{r}') C_2(\mathbf{r}'', \mathbf{r}') d\mathbf{r}'' + \frac{\tau}{\tau_v} \Pi_v \int P_{sv}(\mathbf{r}, \mathbf{r}') C_1(\mathbf{r}'', \mathbf{r}') d\mathbf{r}'' \quad (20c)$$

To solve integral equations (20) we use approach²⁰ based on Kawabata theory²¹ and rewrite them in the

and the matrix Π_v defined as $\Pi_v = \text{diag}\{-1, 1, 1, -1\}$.

Product of two Green functions (13) in the product space basis given in Table I in given by block-diagonal matrix with 4×4 blocks $P_{sv}(\mathbf{r}, \mathbf{r}')$ similar to the single-valley case:²⁰

$$P_{sv}(\mathbf{r}, \mathbf{r}') = \frac{P_0(\mathbf{r}, \mathbf{r}')}{2} \begin{bmatrix} 1 & in_- & -in_- & n_-^2 \\ -in_+ & 1 & -1 & -in_- \\ in_+ & -1 & 1 & in_- \\ n_+^2 & in_+ & -in_+ & 1 \end{bmatrix}, \quad (17)$$

$$P_0(\mathbf{r}, \mathbf{r}') = \frac{e^{-|\mathbf{r}-\mathbf{r}'|/\ell'}}{2\pi\ell|\mathbf{r}-\mathbf{r}'|} \exp\left[-i\frac{(x+x')(y-y')}{\ell_B^2}\right]. \quad (18)$$

Due to the block structure of Cooperon equation kernel, we may rewrite a single 16×16 matrix equation (12) as a system of equations for 4×4 blocks defined as

$$C(\mathbf{r}, \mathbf{r}') = \begin{pmatrix} C_0(\mathbf{r}, \mathbf{r}') & 0 & 0 & 0 \\ 0 & C_1(\mathbf{r}, \mathbf{r}') & -C_2(\mathbf{r}, \mathbf{r}') & 0 \\ 0 & -C_2(\mathbf{r}, \mathbf{r}') & C_1(\mathbf{r}, \mathbf{r}') & 0 \\ 0 & 0 & 0 & C_0(\mathbf{r}, \mathbf{r}') \end{pmatrix} \quad (19)$$

basis

$$\Phi_{N \geq 1, k}(\mathbf{r}) = \frac{1}{\sqrt{2}} \begin{pmatrix} 0 & \sqrt{2}\phi_{N-1, k} & 0 & 0 \\ \phi_{N, k} & 0 & \phi_{N, k} & 0 \\ \phi_{N, k} & 0 & -\phi_{N, k} & 0 \\ 0 & 0 & 0 & -\sqrt{2}\phi_{N+1, k} \end{pmatrix}, \quad (21a)$$

$$\Phi_{0, k}(\mathbf{r}) = \frac{1}{\sqrt{2}} \begin{pmatrix} 0 & 0 & 0 & 0 \\ \phi_{0, k} & 0 & \phi_{0, k} & 0 \\ \phi_{0, k} & 0 & -\phi_{0, k} & 0 \\ 0 & \sqrt{2}\phi_{0, k} & 0 & -\sqrt{2}\phi_{1, k} \end{pmatrix}. \quad (21b)$$

where $\phi_{N,k}$ are the oscillator functions of particle with double charge in the Landau gauge.

Product of two Green functions (13) is convenient to write in the basis (21) as

$$P(\mathbf{r}, \mathbf{r}') = \frac{\tau'}{\tau} \sum_{N,k} \Phi_{Nk}(\mathbf{r}) P_N \Phi_{Nk}^\dagger(\mathbf{r}'). \quad (22)$$

Straightforward calculation with the use of results presented in Appendix C gives the following result for the decomposition of (13) in the basis (21):

$$P_{N \geq 1} = \epsilon \begin{pmatrix} 0 & 0 & 0 & 0 \\ 0 & P_{N-1}^0 & -iP_N^1 & -P_{N+1}^2 \\ 0 & -iP_N^1 & P_N^0 & -iP_{N+1}^1 \\ 0 & -P_{N+1}^2 & -iP_{N+1}^1 & P_{N+1}^0 \end{pmatrix} \epsilon, \quad (23a)$$

$$P_0 = \epsilon \begin{pmatrix} 0 & 0 & 0 & 0 \\ 0 & P_0^0 & 0 & 0 \\ 0 & 0 & P_0^0 & -iP_1^1 \\ 0 & 0 & -iP_1^1 & P_1^0 \end{pmatrix} \epsilon. \quad (23b)$$

Here for brevity we introduced auxiliary matrix $\epsilon = \text{diag}\{1, 1/\sqrt{2}, 1, 1/\sqrt{2}\}$. Integrals P_N^M are given by

$$P_N^M = \frac{\ell_B}{\ell'} \sqrt{\frac{(N-M)!}{N!}} \times \int_0^\infty \exp\left[-x \frac{\ell_B}{\ell'} - \frac{x^2}{2}\right] L_{N-M}^{(M)}(x^2) x^M dx, \quad (24)$$

where $L_{N-M}^{(M)}$ are the Laguerre polynomials. Note that (24) (see also (A1)) slightly differs from definition of similar integrals used in Refs. 20–22 to simplify analysis of its properties and numerical calculations, see Appendix A.

Then it is easy to show that by substitution

$$C_\alpha(\mathbf{r}, \mathbf{r}') = W \sum_{N, k_y} \Phi_{N, k_y}(\mathbf{r}) C_{\alpha N} \Phi_{N, k_y}^\dagger(\mathbf{r}'), \quad (25)$$

we transform integral equations (20) into system of linear equations which allows to find Cooperons:

$$C_{0N} = 1 + \frac{\tau'}{\tau} P_N C_{0N}, \quad (26a)$$

$$C_{1N} = 1 + \frac{\tau'}{\tau} P_N C_{1N} + \frac{\tau'}{\tau_v} \Pi P_N C_{2N} \quad (26b)$$

$$C_{2N} = \frac{\tau}{\tau_v} \Pi + \frac{\tau'}{\tau} P_N C_{2N} + \frac{\tau'}{\tau_v} \Pi P_N C_{1N} \quad (26c)$$

where matrix Π is a matrix Π_v in the basis (21): $\Pi = \text{diag}\{1, -1, 1, -1\}$ with solution

$$C_{0N} = \left(1 - \frac{\tau'}{\tau} P_N\right)^{-1}, \quad (27a)$$

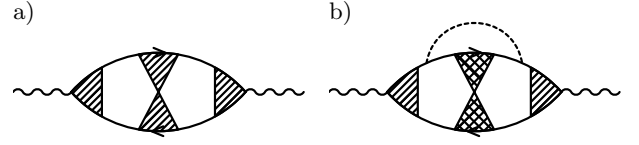


FIG. 3. Standard diagrams which give main contribution to the weak localization.

$$\begin{pmatrix} C_{1N} \\ C_{2N} \end{pmatrix} = \begin{pmatrix} 1 - \frac{\tau'}{\tau} P_N & -\frac{\tau'}{\tau_v} \Pi P_N \\ -\frac{\tau'}{\tau_v} \Pi & 1 - \frac{\tau'}{\tau} P_N \end{pmatrix}^{-1} \begin{pmatrix} 1 \\ \frac{\tau}{\tau_v} \Pi \end{pmatrix} \quad (27b)$$

Note that low magnetic field limit (see below) of these equations is exactly equal to non-diffusion approximation in zero magnetic field given in Ref. 8. Basis choice in Table I makes the form of all equations consistent with non-diffusion theory in zero magnetic field.⁸

In the following, for the conductivity calculations we will need equations associated with fan diagrams starting from two or three scatterers, while our definition (see Fig. 1), which is more convenient for Cooperon equation solution, gives sum of fan diagrams starting from single scattering. To add one or two scatterings, one needs to multiply the result (27a) to kernel of Cooperon equation:

$$C_{0N}^{(m)} = \left(\frac{\tau'}{\tau} P_N\right)^{m-1} C_{0N}, \quad (28a)$$

$$\begin{pmatrix} C_{1N}^{(m)} \\ C_{2N}^{(m)} \end{pmatrix} = \begin{pmatrix} \frac{\tau'}{\tau} P_N & \frac{\tau'}{\tau_v} \Pi P_N \\ \frac{\tau'}{\tau_v} \Pi & \frac{\tau'}{\tau} P_N \end{pmatrix}^{m-1} \begin{pmatrix} C_{1N} \\ C_{2N} \end{pmatrix} \quad (28b)$$

Equations (27), (28) allow easily compute Cooperons in the basis (21).

C. Conductivity correction

A consistent theory of weak localization is developed in the framework of the diagram technique. The weak-localization corrections to the conductivity arise in the first order of the parameter $(k_F \ell)^{-1}$. The weak localization correction to conductivity has two contributions corresponding to standard diagrams illustrated in Fig. 3 (see Refs. 22 and 23 for details). It may be shown that all other diagrams either have higher in $(k_F \ell)^{-1}$ order or do not depend on τ_ϕ which defines the magneto and temperature dependence of the conductivity correction.

It may be shown that first diagram may be written as

$$\sigma_a = \frac{\hbar}{2\pi} \int \text{Tr} \left[F(\mathbf{r}, \mathbf{r}') \mathcal{C}^{(3)}(\mathbf{r}', \mathbf{r}) \right] d\mathbf{r} d\mathbf{r}', \quad (29)$$

where $F(\mathbf{r}, \mathbf{r}') = J_x(\mathbf{r}, \mathbf{r}') \otimes J_x(\mathbf{r}, \mathbf{r}')$, $\mathbf{J}(\mathbf{r}, \mathbf{r}')$ is the combination of dressed current vertex with Green functions $\mathbf{J}(\mathbf{r}, \mathbf{r}') = \int G(\mathbf{r}, \mathbf{r}_1) \mathbf{j}(\mathbf{r}_1, \mathbf{r}_2) G(\mathbf{r}_2, \mathbf{r}')$. Bare vertex is velocity operator which may be written as

$$\mathbf{j}_0 = ev \begin{pmatrix} \sigma & 0 \\ 0 & -\sigma \end{pmatrix} \delta(\mathbf{r} - \mathbf{r}') \quad (30)$$

Evaluation analogous to one given in Ref. 8 gives similar result

$$\mathbf{j} = 2ev \begin{pmatrix} \boldsymbol{\sigma} & 0 \\ 0 & -\boldsymbol{\sigma} \end{pmatrix} \delta(\mathbf{r} - \mathbf{r}') \quad (31)$$

It should be noted that (31) assumes $\tau_\phi \gg \tau$, but has no restrictions on τ_v compared with τ .

Direct evaluation with the help of equations given in Appendix C for a dressed current leads to

$$J^\pm(\mathbf{r}, \mathbf{r}') = \pm e \frac{\sqrt{2}\ell'}{\hbar} n_\pm [G^R(\mathbf{r}, \mathbf{r}') + G^A(\mathbf{r}, \mathbf{r}')] \quad (32)$$

To write conductivity correction using solution of Cooperon equation obtained earlier we should rewrite $F(\mathbf{r}, \mathbf{r}')$ in the ‘‘product space basis’’. In the following it is important to note that F in the conductivity correction is integrated and in the product terms $[G^{R,A}(\mathbf{r}, \mathbf{r}')]^2$ are small compared to $G^{R/A}(\mathbf{r}, \mathbf{r}')G^{A/R}(\mathbf{r}, \mathbf{r}')$ because of the smallness of $(k_F\ell)^{-1}$.

Also it is important that current has a n_\pm as a multiplier. It leads to zero off-diagonal components of current $\sigma_{+-} = \sigma_{-+} = 0$

Finally, we may rewrite product of two Green functions using (13) which gives

$$\sigma_a = -\frac{e^2\ell'^2}{\pi\hbar} \sum_{\alpha\beta\gamma\delta} \int \frac{1}{2W} [P_{\beta\gamma}^{\delta\alpha}(\mathbf{r}, \mathbf{r}') + P_{\delta\alpha}^{\beta\gamma}(\mathbf{r}, \mathbf{r}')] \left\{ \mathcal{C}^{(3)} \right\}_{\gamma\delta}^{\alpha\beta}(\mathbf{r}', \mathbf{r}) \quad (33)$$

which with the definition

$$Q_{\delta\gamma}^{\beta\alpha} = -\frac{P_{\beta\gamma}^{\delta\alpha}(\mathbf{r}, \mathbf{r}') + P_{\delta\alpha}^{\beta\gamma}(\mathbf{r}, \mathbf{r}')}{2} \quad (34)$$

may be written as

$$\sigma_a = \frac{e^2\ell'^2}{\pi\hbar} \sum_{\alpha\beta\gamma\delta} \int \frac{1}{W} Q_{\delta\gamma}^{\beta\alpha}(\mathbf{r}, \mathbf{r}') \left\{ \mathcal{C}^{(3)} \right\}_{\gamma\delta}^{\alpha\beta}(\mathbf{r}', \mathbf{r}). \quad (35)$$

Exchange of couple left(right) indices in one-particle space in the product space chose in accordance with the Table I is equivalent to multiplication from the left (right) to the matrix

$$\Pi_* = \begin{pmatrix} \Pi_r & 0 & 0 & 0 \\ 0 & 0 & \Pi_r & 0 \\ 0 & \Pi_r & 0 & 0 \\ 0 & 0 & 0 & \Pi_r \end{pmatrix}, \quad (36)$$

where

$$\Pi_r = \begin{pmatrix} 1 & 0 & 0 & 0 \\ 0 & 0 & 1 & 0 \\ 0 & 1 & 0 & 0 \\ 0 & 0 & 0 & 1 \end{pmatrix}. \quad (37)$$

It is then essential to take advantage from the block structure of $P(\mathbf{r}, \mathbf{r}')$ and Π_* which allows one to rewrite Q in a product space as

$$Q(\mathbf{r}, \mathbf{r}') = \begin{pmatrix} Q_{sv}(\mathbf{r}, \mathbf{r}') & 0 & 0 & 0 \\ 0 & 0 & Q_{sv}(\mathbf{r}, \mathbf{r}') & 0 \\ 0 & Q_{sv}(\mathbf{r}, \mathbf{r}') & 0 & 0 \\ 0 & 0 & 0 & Q_{sv}(\mathbf{r}, \mathbf{r}') \end{pmatrix}, \quad (38)$$

with

$$Q_{sv}(\mathbf{r}, \mathbf{r}') = -\frac{\Pi_r P_{sv}(\mathbf{r}, \mathbf{r}') + P_{sv}(\mathbf{r}, \mathbf{r}') \Pi_r}{2}. \quad (39)$$

Then we use block form if the Cooperons (19) and rewrite these equations as

$$\sigma_a = 2 \frac{e^2}{\pi\hbar} \frac{\ell'^2}{W} \int \text{Tr} \{ Q_{sv}(\mathbf{r}, \mathbf{r}') [C_0(\mathbf{r}', \mathbf{r}) - C_2(\mathbf{r}', \mathbf{r})] \} \quad (40)$$

For the computation, we decompose (40) in the basis (21):

$$Q_{sv}(\mathbf{r}, \mathbf{r}') = \sum_{N,k} \Phi_{Nk}(\mathbf{r}) Q_N \Phi_{Nk}^\dagger(\mathbf{r}'), \quad (41)$$

It may be shown that

$$Q_N = \frac{\Pi' P_N + P_N \Pi'}{2} \quad (42)$$

Where Π' is the matrix similar to Π defined in Eq. (26), it is a $-\Pi_r$ in the basis (21): $\Pi' = \text{diag} \{-1, -1, 1, -1\}$. Note opposite sign which we introduced to make Π' and Π coincide with matrix defined in Ref. 8.

And the final result for the weak localization correction associated with diagram Fig. 3(a) is given by

$$\sigma_a = 2 \frac{e^2}{\pi^2\hbar} \frac{2\ell'^2}{\ell_B^2} \sum_N \text{Tr} \left\{ Q_N [C_{0N}^{(3)} - C_{2N}^{(3)}] \right\}. \quad (43)$$

Note that the result (43) is extremely similar to weak localization correction in non-diffusion theory in zero magnetic field. Moreover, accurate calculation of zero magnetic field limit as a formal limit $\ell/\ell_B \rightarrow 0$ gives the result which is exactly equal to results presented in Ref. 8. The notation in the current manuscript is chosen to simplify this comparison. As explained in Appendix B, in addition it facilitates the use of low field limit for precise computation of slowly converging infinite sum (43).

For the diagrams of type (b) evaluation of conductivity correction is more complicated. We will formulate it using definition

$$L^\pm(\mathbf{r}, \mathbf{r}') = \pm n_\pm P(\mathbf{r}, \mathbf{r}') \quad (44)$$

which originates from combination of dressed current and Green function

$$\begin{aligned} e \frac{\sqrt{2}\ell'}{\hbar} \{ L^j \}_{\gamma\delta}^{\alpha\beta}(\mathbf{r}, \mathbf{r}') &\simeq J_{\alpha\beta}^j(\mathbf{r}, \mathbf{r}') G_{\gamma\delta}^R(\mathbf{r}, \mathbf{r}') \\ &\simeq J_{\gamma\delta}^j(\mathbf{r}, \mathbf{r}') G_{\alpha\beta}^A(\mathbf{r}, \mathbf{r}') \end{aligned} \quad (45)$$

where sign \simeq is used to show the equivalence up to terms proportional to $(k_F \ell)^{-1}$ in the conductivity.

With this definition conductivity may be written as (note that there are two diagrams with scattering "above" and "below" Cooperon)

$$\sigma_b^{ij} = \frac{e^2}{2\pi} \frac{2\ell'^2}{\hbar^2} \int \text{Tr} \left\{ L^i(\mathbf{r}', \mathbf{r}_1) S \Pi_* L^j(\mathbf{r}_1, \mathbf{r}) C^{(2)}(\mathbf{r}, \mathbf{r}') + L^j(\mathbf{r}', \mathbf{r}_1) S \Pi_* L^i(\mathbf{r}_1, \mathbf{r}) C^{(2)}(\mathbf{r}, \mathbf{r}') \right\} \quad (46)$$

By using block form of matrices we may write this result as

$$\sigma_b^{ij} = 2 \frac{e^2}{\pi} \frac{\ell'^2}{\hbar^2} \int \text{Tr} \left\{ L_{sv}^i(\mathbf{r}', \mathbf{r}_1) \Pi_r L_{sv}^j(\mathbf{r}_1, \mathbf{r}) [C_0(\mathbf{r}, \mathbf{r}') - C_2(\mathbf{r}, \mathbf{r}')] \right. \\ \left. - \frac{\tau}{\tau_v} L_{sv}^i(\mathbf{r}', \mathbf{r}_1) \Pi_v \Pi_r L_{sv}^j(\mathbf{r}_1, \mathbf{r}) C_1(\mathbf{r}, \mathbf{r}') \right\} + i \leftrightarrow j \quad (47)$$

For the computation, we rewrite L^\pm in the basis (21). Direct calculation with the use of Appendix C gives

$$L_{sv}^+(\mathbf{r}, \mathbf{r}') = i \sum_k \left[\Psi_{0k}(\mathbf{r}) L_0^T \Psi_{0k}^\dagger(\mathbf{r}') + \sum_N \Psi_{N+1,k}(\mathbf{r}) L_{N+1}^T \Psi_{Nk}^\dagger(\mathbf{r}') \right] \quad (48a)$$

$$L_{sv}^-(\mathbf{r}, \mathbf{r}') = i \sum_k \left[\Psi_{0k}(\mathbf{r}) L_0 \Psi_{0k}^\dagger(\mathbf{r}') + \sum_N \Psi_{Nk}(\mathbf{r}) L_{N+1} \Psi_{N+1,k}^\dagger(\mathbf{r}') \right] \quad (48b)$$

where we defined (technically, we have to compute L_1 separately, but the result is the same as for $L_{N \geq 2}$ setting $P_N^M = 0$ for $M > N$)

$$L_{N \geq 1} = \epsilon \begin{pmatrix} 0 & 0 & 0 & 0 \\ 0 & -iP_{N-1}^1 & -P_N^2 & iP_{N+1}^3 \\ 0 & P_{N-1}^0 & -iP_N^1 & -P_{N+1}^2 \\ 0 & -iP_N^1 & P_N^0 & -iP_{N+1}^1 \end{pmatrix} \epsilon \quad (49a)$$

$$L_0 = \epsilon \begin{pmatrix} 0 & 0 & 0 & 0 \\ 0 & 0 & -P_0^0 & iP_1^1 \\ 0 & 0 & 0 & 0 \\ 0 & 0 & 0 & 0 \end{pmatrix} \epsilon \quad (49b)$$

One may note that $\sigma_b^{++} = \sigma_b^{--} = 0$ and $\sigma_b^{+-} = \sigma_b^{-+} \equiv \sigma_b$.

Analogously to σ_a , we arrive to the following equation

for σ_b :

$$\sigma_b = \frac{e^2}{\pi^2 \hbar} \frac{2\ell'^2}{\ell_B^2} \text{Tr} \left\{ L_0 \Pi' L_0^T [C_{00}^{(2)} - C_{20}^{(2)}] - \frac{\tau}{\tau_v} L_0 \Pi \Pi' L_0^T C_{10}^{(2)} \right. \\ \left. + \sum_N [L_N^T \Pi' L_N + L_{N+1} \Pi' L_{N+1}^T] [C_{0N}^{(2)} - C_{2N}^{(2)}] \right. \\ \left. - \frac{\tau}{\tau_v} [L_N^T \Pi \Pi' L_N + L_{N+1} \Pi \Pi' L_{N+1}^T] C_{1N}^{(2)} \right\} \quad (50)$$

The structure of the answer is very close to the one obtained in Ref. 8 with integration is replaced with a summation over Landau levels. The only significant discrepancy is an extra term for 0-th Landau level.

Note that for a chosen scattering contribution to the conductivity from the singlet is zero. Practical computation may assume all computations for 3×3 block in matrices. For completeness we left singlet contribution in all equations to avoid possible confusion.

D. Low magnetic field limit

In the above, we assumed classically weak magnetic fields $k_F \ell_B \gg 1$. This allowed us following Kawabata²¹ to factorize electron Green function into zero-field Green function and phase factor which absorbs the effect of magnetic field.

Diffusion pole in Cooperon equation is cut off by phase relaxation time which means that infinite sum in (43), (50) is defined by $N \gg 1$ and N may be correctly replaced with integration over continuous variable if $\ell^2/2\ell_B^2 \gg \tau_\phi/\tau$. Only for such small magnetic fields the we may replace summation with the integration assuming N large.

In this case, we may find P_N^M (24) in elementary functions by using Mehler-Heine asymptotic for Laguerre

polynomials

$$L_N^{(M)}(x \rightarrow 0) \rightarrow e^{\frac{\pi}{2}} \left(\frac{N}{x}\right)^{\frac{M}{2}} J_M(2\sqrt{xN}) \quad (51)$$

$$P_N^M(\alpha) = (-i)^M I_M \left(\frac{2\sqrt{N}}{\alpha} \right), \quad (52)$$

$$I_M(q) = \frac{[\sqrt{1+q^2}-1]^M}{q^M \sqrt{1+q^2}}$$

And the summation may be replaced with integration using the following rule:

$$\sum_N f(N) \rightarrow \frac{\ell_B^2}{2} \int_0^\infty f(N = q^2 \ell_B^2/4) q dq \quad (53)$$

Following this procedure, we may obtain non-diffusion results for the weak localization correction⁸ from (43), (50).

IV. RESULTS

Fig. 4 is the main result of our work and it shows the transition from weak antilocalization to the weak localizations when changing the intervalley transitions rate. Curve 1 corresponds to the absence of intervalley transitions, in this case zero field contribution to the quantum correction is positive (WAL) and conduction decreases as a function of magnetic field. Curve 2 corresponds to the case when intervalley transitions time is equal to the phase decoherence time in one Dirac cone. In this case WAL survives, but quantum correction decreases. Increase of intervalley transitions as compared to loss of coherency in one valley leads to further suppression of the quantum correction in zero magnetic field and to non monotonous dependence of the conductivity as a function of magnetic field. The latter is caused by the fact that when magnetic length ℓ_B becomes comparable with diffusion length ℓ , the WAL correction is suppressed in comparison with the decoherence time in one valley. Further decrease of intervalley transitions in 50 and 100 times as compared to τ_ϕ leads to the change of quantum correction sign which results in “restore” of the time-reversal symmetry and necessity to take into account states of the both valleys when considering the carriers scattering. Curve 4 has an extremum point yet, but curve 5 finally corresponds to “conventional” magnetoresistance caused by the weak localization.

Intervalley contribution to the conductivity due to its time-invariant nature results in a conventional WL, similar to spinless single valley case. However, it is proportional to the intervalley scattering rate. Without intervalley scattering, when trigonal warping and reduced symmetry scatterers may be neglected, the intravalley contribution comes into play. Due to Berry phase which

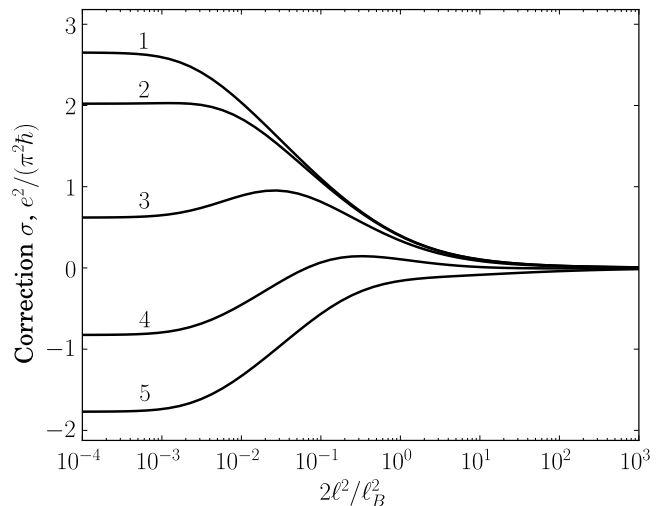


FIG. 4. Weak localization correction as a function of magnetic field. Here $\frac{\tau}{\tau_\phi} = 10^{-3}$ and $\frac{\tau}{\tau_v} = 0.0, 10^{-3}, 10^{-2}, 0.05, 0.1$ (labelled as 1, 2, 3, 4, 5 correspondingly).

originates from the structure of the wavefunctions intravalley scattering introduces additional phase which results in opposite sign of conductivity correction.^{6,9,20} Controlling the intervalley scattering rate one may continuously switch between two cases.

Results presented in Fig. 4 demonstrate that the change of localization correction sign takes place at relatively effective intervalley transitions, when the phase relaxation time in one valley is about two orders of magnitude longer than these transitions, but the condition $\tau_\phi > \tau_v \gg \tau$ still holds. In the Ref. 24 the transition from WL to WAL has been observed in graphene when the carrier concentration has been decreased. In the framework of the theory developed here these results may be interpreted as a change of the ratio τ_ϕ/τ_v as a function of carrier concentration.

Non monotonous dependence of conductivity as a function of magnetic field (curve 3) for a region of τ_v/τ_ϕ ratio is a characteristic property of two-dimensional graphene layers defined by its band structure. Similar behaviour of $\sigma(B)$ has not been observed in other multivalley systems, e.g. Si.¹⁴

To conclude, we have developed the theory of the weak localization in graphene with account on intervalley transitions in the whole range of classically weak magnetic fields. It has been shown that in two-dimensional graphene layers intervalley transitions lead to crossover between weak antilocalization and weak localization regimes and all peculiarities of the system are defined by spinor-like character of carrier wavefunctions. Spin-orbit interaction and suppression of backscattering in quantum relaxation time are shown to be virtually unimportant in the theoretical description of the weak localization in graphene. In addition, we have developed a novel analytical approach for the calculation of weak localization in the systems with linear spectrum which allows to simplify

conceptually the numerical calculation of quantum correction to the conductivity in non-zero magnetic fields.

Appendix A: Numerical calculation of $P_N^M(x)$

In this section we comment on numerical computation of integrals (in this section we sometimes omit function argument α for brevity)

$$P_N^M(\alpha) = \alpha \sqrt{\frac{(N-M)!}{N!}} \int e^{-\alpha\zeta - \frac{1}{2}\zeta^2} \zeta^M L_{N-M}^M(\zeta^2) d\zeta. \quad (\text{A1})$$

Laguerre polynomials for large N are highly oscillating functions, and straightforward numerical integration using (A1) is impractical. Moreover, if one wants to use this definition to compute $P_N^M(\alpha)$, for large integration variable exponent underflows and Laguerre polynomial overflows, despite the fact that their product is finite and well defined. The latter problem may be overcome by redefining integrand via Laguerre function $e^{-x/2} x^{M/2} L_{N-M}^M(x)$ and calculating this function using recurrent relation

which may be easily derived from recurrence relations for Laguerre polynomials. However, there exists a more efficient approach which allows to obtain the functions (A1) with negligible computational complexity.

As shown in Kawabata’s work,²¹ Laguerre integrals (A1) with $M = 0$ satisfy four-term recurrence relation

$$P_0^0(\alpha) = \alpha \sqrt{\frac{\pi}{2}} \exp\left(\frac{\alpha^2}{2}\right) \operatorname{erfc}\left(\frac{\alpha}{\sqrt{2}}\right), \quad (\text{A2a})$$

$$P_1^0(\alpha) = \alpha^2 - \alpha^2 P_0(\alpha), \quad (\text{A2b})$$

$$P_2^0(\alpha) = \frac{1 + \alpha^2}{2} [P_0(\alpha) - P_1(\alpha)], \quad (\text{A2c})$$

$$P_N^0(\alpha) = \frac{N-2}{N} P_{N-3}(\alpha) + \frac{N-1 + \alpha^2}{N} [P_{N-2}(\alpha) - P_{N-1}(\alpha)]. \quad (\text{A2d})$$

It may be shown that this recurrence relation is numerically unstable. For computations one may rewrite recurrence relation (A2) as a system of linear equations with banded matrix²⁵

$$\begin{pmatrix} a_4 & 1 & & & & & & & & \\ -a_5 & a_5 & 1 & & & & & & & \\ b_6 & -a_6 & a_6 & & 1 & & & & & \\ & \ddots & \ddots & \ddots & \ddots & \ddots & & & & \\ & & b_{N_{max}-1} & -a_{N_{max}-1} & a_{N_{max}-1} & & & & & \\ & & & b_{N_{max}} & -a_{N_{max}} & a_{N_{max}} & & & & \\ & & & & & & & & & 1 \end{pmatrix} \begin{pmatrix} P_3^0 \\ P_4^0 \\ P_5^0 \\ \vdots \\ P_{N_{max}-2}^0 \\ P_{N_{max}-1}^0 \end{pmatrix} = \begin{pmatrix} -b_4 P_1^0 + a_4 P_2^0 \\ -b_5 P_2^0 \\ 0 \\ \vdots \\ 0 \\ -P_{N_{max}}^0 \end{pmatrix}, \quad (\text{A3})$$

where

$$a_n = \frac{n-1 + \alpha^2}{n}, \quad b_n = -\frac{n-2}{n}, \quad (\text{A4})$$

and $P_{N_{max}}^0$ may be taken from approximation for large N

$$P_N^0(\alpha) \xrightarrow{N \rightarrow \infty} \frac{1}{\sqrt{1 + \frac{4(N+1/2)}{\alpha^2}}}. \quad (\text{A5})$$

Note that the numerical error due to use of approximated value for $P_{N_{max}}^0$ exponentially decays for small N and the result is exact for $N < N_{max} - \delta N$ where δN is relatively small.

For $M \neq 0$ we define scaled integrals

$$P_n^1 = \frac{\alpha}{\sqrt{n}} \tilde{P}_n^1, \quad (\text{A6a})$$

$$P_n^2 = \frac{1}{\sqrt{(n-1)n}} \tilde{P}_n^2, \quad (\text{A6b})$$

$$P_n^3 = \frac{\alpha}{\sqrt{(n-2)(n-1)n}} \tilde{P}_n^3, \quad (\text{A6c})$$

which satisfy the following recurrences:

$$\tilde{P}_n^1 = \tilde{P}_{n-2}^1 - P_{n-1}^0 + P_{n-2}^0, \quad (\text{A7a})$$

$$\tilde{P}_n^2 = 1 + \tilde{P}_{n-2}^2 - (1 + \alpha^2) \tilde{P}_{n-1}^1 - (1 - \alpha^2) \tilde{P}_{n-2}^1, \quad (\text{A7b})$$

$$\tilde{P}_n^3 = \tilde{P}_{n-2}^3 + 2\tilde{P}_{n-2}^1 - \tilde{P}_{n-1}^2 + \tilde{P}_{n-2}^2. \quad (\text{A7c})$$

with additional initial values

$$\tilde{P}_1^1 = -P_1^0 + P_0^0, \quad (\text{A7d})$$

$$\tilde{P}_{n < M}^M = 0. \quad (\text{A7e})$$

It is worth to note that approach (A3-A7) needs only $\mathcal{O}(N)$ floating point operations to compute $4N$ functions $P_{n < N}^{M=0,1,2,3}(\alpha)$ for each argument α . This is negligible compared with $\mathcal{O}(N^3)$ operations to compute them using (A1). If one is interested in benchmarking recurrent approach (A3-A7), it is practical to compare it with “reference” values calculated by definition (A1) (taking into account remark about the Laguerre function computation) to estimate necessary N_{max} and δN as a functions of α to obtain any desired accuracy.

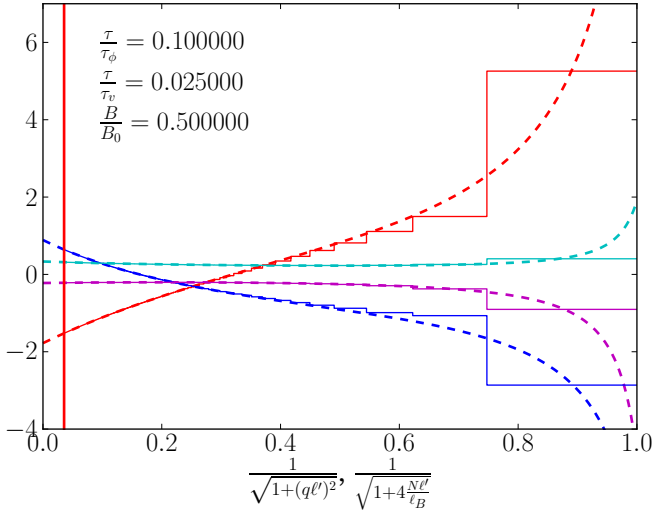


FIG. 5. Illustration of accurate summation by using nondiffusion approximation for large values of Landau level number. Contributions to the weak localization correction calculated using (43), (50) are compared with non-diffusion approximation⁸ after changing integration variable to $I = 1/\sqrt{1+(q\ell')^2}$. For comparison, we treat sum as an integral of almost everywhere constant function of real variable N and change the variable to $1/\sqrt{1+(2N\ell'/\ell_B)^2}$. Intravalley and intervalley contributions from diagrams of type (a) and (b) are shown separately. Vertical line shows position of 1000th Landau level. For an accurate computation, we use sum for $N < 1000$ and integral for $N \geq 1000$

Appendix B: Numerical calculation of infinite sums in conductivity

Conductivity correction written as a sum over Landau level converges extremely slowly, it is easy to show that

$$\sum_{N_{max}}^{\infty} \sim \mathcal{O}\left(\frac{1}{\sqrt{N_{max}}}\right), \quad (\text{B1})$$

which makes it technically complicated to evaluate sums in Eqs. (43), (50) with reasonable precision. For realistic calculations the convergence of these sums may be significantly improved: if the infinite sum remainder is approximated by the low magnetic field limit, then it is easy to show that

$$\sum_{N_{max}}^{\infty} - \int_{N_{max}}^{\infty} \sim \mathcal{O}\left(\frac{1}{N_{max}}\right). \quad (\text{B2})$$

This crucially improves convergence of infinite sums. Similar approach is mentioned briefly in Ref. 26.

To illustrate this approximation, in Fig. 5 we show weak localization correction contributions separately for $\tau/\tau_\phi = 0.1$, $\tau/\tau_v = 0.025$, $B/B_0 = 2\ell^2/\ell_B^2 = 0.5$. To simplify the comparison the sums (43), (50) may be written as integrals of piecewise constant functions of continuous N . These functions are shown in Fig. 5 in solid lines and

their approximation with low magnetic field limit (see Sec. III D) are shown in dashed lines.

Mathematically, it is clear that the low field limit is based not on the large compared with unity value of $N\ell/\ell_B$. For any value of magnetic field, there exists a number N_{max} when (51) gives a good approximation of Laguerre polynomial and summation may be replaced with the integration.

Physically, effect of magnetic field on large trajectories is always diffusion-like. It is a matter of the size of a trajectory compared with magnetic length, when the trajectory may be considered “large”.

Appendix C: Some integral and sums

In the manuscript, we used some mathematical facts which are given here for completeness. In the manuscript we use definitions:

$$\boldsymbol{\rho} = \mathbf{r} - \mathbf{r}', \quad n_{\pm} = \frac{\rho_x \pm i\rho_y}{|\boldsymbol{\rho}|} \quad (\text{C1})$$

All infinite sums for single-particle basis functions may be derived from the following relation for oscillator functions (5):

$$\sum_{N,k} \frac{\psi_{N,k}(\mathbf{r})\psi_{N-\eta M,k}^*(\mathbf{r}')}{\varepsilon - \hbar\omega_c\sqrt{N} \pm \frac{i\hbar}{2\tau'}} \simeq - \frac{(\mp i\eta n_\eta)^M e^{-i\frac{(x+x')(y-y')}{2\ell_B^2}}}{\hbar v\sqrt{2\pi}\sqrt{\rho/k_F}} e^{-\frac{\rho^2}{2\ell^2}} e^{\pm i(\rho k_F + \pi/4)}. \quad (\text{C2})$$

Here $\eta = \pm 1$.

Equation (C2) may be obtained as a limit $k_F\ell \gg 1$, $k_F\ell_B \gg 1$ of the exact relation

$$\sum_{N,k} \frac{\psi_{N,k}(\mathbf{r})\psi_{N-\eta M,k}^*(\mathbf{r}')}{\varepsilon - \hbar\omega_c\sqrt{N} \pm \frac{i\hbar}{2\tau'}} = \frac{e^{-i\frac{(x+x')(y-y')}{2\ell_B^2}} e^{-\frac{\rho^2}{4\ell_B^2}} \left(\frac{\rho^2}{2\ell_B^2}\right)^{\frac{M}{2}}}{2\pi\hbar v} n_\eta^M \times \frac{1}{\ell_B} \sum_N \sqrt{\frac{(N-M)!}{N!}} \frac{L_{N-M}^M\left(\frac{\rho^2}{2\ell_B^2}\right)}{2\sqrt{N} - (k_F\ell_B \pm i\frac{\ell_B}{2\ell'})} \quad (\text{C3})$$

under additional assumptions $M \sim 1$, $\rho \ll \ell_B^2 k_F$.

Matrix elements of Cooperon kernel in the basis two-particle functions may be derived from matrix elements of $P_0(\mathbf{r}, \mathbf{r}')$ (18) which are obtained by direct calculation

$$\int \phi_{Nk}^*(\mathbf{r}) n_\pm^M P_0(\mathbf{r}, \mathbf{r}') \phi_{N'k'}(\mathbf{r}') = \frac{\ell'}{\ell} \delta_{k,k'} \delta_{N,N' \pm M} (\pm 1)^M P_{\max\{N,N'\}}^M\left(\frac{\ell_B}{\ell'}\right) \quad (\text{C4})$$

where P_N^M defined in (A1)

ACKNOWLEDGMENTS

The authors acknowledge fruitful discussions with L.E. Golub and S.A. Tarasenko. This work was sup-

ported by the RFBR grant 12-02-00580, EU project “POLAPHEN”, RF President Grant NSh-1085.2014.2 and by the Government of Russia through the program P220 (project 14.Z50.31.0021, leading scientist M. Bayer).

-
- ¹ A. K. Geim and K. S. Novoselov, *Nature Mat.* **6**, 183 (2007).
- ² A. H. Castro Neto, F. Guinea, N. M. R. Peres, K. S. Novoselov, and A. K. Geim, *Rev. Mod. Phys.* **81**, 109 (2009).
- ³ G. Tkachov and E. M. Hankiewicz, *physica status solidi (b)* **250**, 215 (2013).
- ⁴ I. V. Gornyi, V. Y. Kachorovskii, A. D. Mirlin, and P. M. Ostrovsky, *physica status solidi (b)* (2014), 10.1002/pssb.201350309.
- ⁵ I. V. Gornyi, V. Y. Kachorovskii, and P. M. Ostrovsky, *arXiv:1402.7097 [cond-mat]*.
- ⁶ H. Suzuura and T. Ando, *Phys. Rev. Lett.* **89**, 266603 (2002).
- ⁷ E. McCann, K. Kechedzhi, V. I. Fal’ko, H. Suzuura, T. Ando, and B. L. Altshuler, *Phys. Rev. Lett.* **97**, 146805 (2006).
- ⁸ M. O. Nestoklon and N. S. Averkiev, *EPL (Europhysics Letters)* **101**, 47006 (2013).
- ⁹ K. Kechedzhi, E. McCann, V. I. Fal’ko, H. Suzuura, T. Ando, and B. L. Altshuler, *The European Physics Journal* **148**, 39 (2007).
- ¹⁰ F. V. Tikhonenko, A. A. Kozikov, A. K. Savchenko, and R. V. Gorbachev, *Phys. Rev. Lett.* **103**, 226801 (2009).
- ¹¹ A. N. Pal, V. Kochat, and A. Ghosh, *Phys. Rev. Lett.* **109**, 196601 (2012).
- ¹² A. M. R. Baker, J. A. Alexander-Webber, T. Altbauer, T. J. B. M. Janssen, A. Tzalenchuk, S. Lara-Avila, S. Kubatkin, R. Yakimova, C.-T. Lin, L.-J. Li, and R. J. Nicholas, *Phys. Rev. B* **86**, 235441 (2012).
- ¹³ N. S. Averkiev and G. E. Pikus, *Physics of the Solid State* **38**, 964 (1996).
- ¹⁴ A. Y. Kuntsevich, N. N. Klimov, S. A. Tarasenko, N. S. Averkiev, V. M. Pudalov, H. Kojima, and M. E. Gershenson, *Phys. Rev. B* **75**, 195330 (2007).
- ¹⁵ M. M. Glazov and L. E. Golub, *Semiconductor Science and Technology* **24**, 064007 (2009).
- ¹⁶ S. V. Morozov, K. S. Novoselov, M. I. Katsnelson, F. Schedin, L. A. Ponomarenko, D. Jiang, and A. K. Geim, *Phys. Rev. Lett.* **97**, 016801 (2006).
- ¹⁷ A. F. Morpurgo and F. Guinea, *Phys. Rev. Lett.* **97**, 196804 (2006).
- ¹⁸ R. Winkler and U. Zülicke, *Phys. Rev. B* **82**, 245313 (2010).
- ¹⁹ G. F. Koster, J. O. Dimmock, R. G. Wheeler, and H. Statz, *The Properties of the Thirty-Two Point Groups* (M.I.T. Press, Cambridge, 1963).
- ²⁰ M. O. Nestoklon, N. S. Averkiev, and S. A. Tarasenko, *Solid State Communications* **151**, 1550 (2011).
- ²¹ A. Kawabata, *Journal of the Physical Society of Japan* **53**, 3540 (1984).
- ²² A. P. Dmitriev, V. Y. Kachorovskii, and I. V. Gornyi, *Phys. Rev. B* **56**, 9910 (1997).
- ²³ V. Gasparian and A. Zyuzin, *Fiz. Tverd. Tela* **27**, 1662 (1985), *sov. Phys. Solid State* **27**, 1580 (1985).
- ²⁴ R. V. Gorbachev, F. V. Tikhonenko, A. S. Mayorov, D. W. Horsell, and A. K. Savchenko, *Phys. Rev. Lett.* **98**, 176805 (2007).
- ²⁵ Note the use of P_1^0 and P_2^0 as a left boundary condition. Surprisingly, this strongly improves precision of the result. Also, in the functions $P_1^0(\alpha)$ and $P_2^0(\alpha)$ at the left boundary for large argument instead of using (A2) one should use series in $1/\alpha$ for a reasonable accuracy.
- ²⁶ A. Cassam-Chenai and B. Shapiro, *J. Phys. I France* **4**, 1527 (1994).